Title

Optimization of scintillator–reflector optical interfaces for the LUT Davis model

Journal

Medical Physics, 48(9)

ISSN

0094-2405

Authors

Trigila, Carlotta
Roncali, Emilie

Publication Date

2021-09-01

DOI

10.1002/mp.15109

Peer reviewed

HHS Public Access

Author manuscript

Med Phys. Author manuscript; available in PMC 2022 September 01.

Published in final edited form as:

Med Phys. 2021 September ; 48(9): 4883–4899. doi:10.1002/mp.15109.

Optimization of scintillator-reflector optical interfaces for the LUT Davis model

Carlotta Trigila[1,a], **Emilie Roncali**[1,2]

[1]Department of Biomedical Engineering, University of California Davis, Davis, CA, United States of America

[2]Department of Radiology, University of California Davis, Davis, CA, United States of America

Abstract

Purpose: Designing and optimizing scintillator-based gamma detector using Monte Carlo simulation is of great importance in nuclear medicine and high energy physics. In scintillation detectors, understanding the light transport in the scintillator and the light collection by the photodetector plays a crucial role in achieving high performance. Thus, accurately modeling them is critical.

Methods: In previous works, we developed a model to compute crystal reflectance from the crystal 3D surface measurement and store it in Look-up Tables to be used in the Monte Carlo simulation software GATE. The relative light output comparison showed excellent agreement between simulations and experiments for both polished and rough surfaces in several configurations, i.e., without and with reflector. However, when comparing them at the irradiation depth closest to the photodetector face, rough crystals with a reflector overestimated the predicted light output.

Investigating the cause of this overestimation, we optimized the LUT algorithm to improve the reflectance computation accuracy, especially for rough surfaces. However, optical Monte Carlo simulations carried out with these newly generated LUTs still overestimate the light output. Based on previous observations, one probable cause is the erroneous assumption of perfect couplings between the reflector and crystal and between the crystal and photodetector, which likely results in an important overestimation of the light output compared to experimental values. In practice, several factors could degrade it. Here, we investigated possible suboptimal optical experimental configurations that could lead to a degraded light collection when using Teflon or ESR reflectors coupled to the crystal with air or grease. We generated look-up tables with a mixture of air and grease and showed the effect of three possible sources of light loss: the presence of a small gap between the crystal and the reflector edges close to the photodetector face, the infiltration of grease in the crystal-reflector coupling, and the presence of inhomogeneities in the photodetector-crystal interface.

[a]Corresponding author: Carlotta Trigila, The Genome and Biomedical Sciences Facility, University of California Davis, 451 Health Sciences Dr., Davis, CA 95616, United States of America. ctrigila@ucdavis.edu.

The authors have no conflict to disclose.

Data Availability Statement

The data that support the findings of this study are available from the corresponding author upon reasonable request.

Results: The strongest effect is linked to the presence of a small gap of grease between the edges of the reflector material and the crystal (light loss of 10–12% for 0.2 mm gap). The optical grease infiltrating the crystal-reflector air coupling decreases the light output, depending on the infiltration's extent and the amount of grease infiltrated. 5% of air in the crystal-photodetector coupling can cause a light output decrease of 2% to 4%. The individual and combined effect of these advanced models can explain the discrepancy of the relative light output obtained with ESR in simulations and experiments. With Teflon, the study indicates that the light output loss strongly depends on the reflectance deterioration caused by grease absorption.

Conclusions: Our results indicate that when studying scintillation detector performance with different finishes, performing simulations in ideal coupling conditions can lead to light output overestimation. To perform an accurate light output comparison and ultimately have a reliable detector performance estimation, all potential sources of practical limitations must be carefully considered. To broadly enable high-fidelity modeling, we developed an interface for users to compute their own LUTs, using their surface, scintillator and reflector characteristics.

Keywords

scintillation detectors; diagnostic imaging; GATE; GEANT4; Monte Carlo optical simulation; surface finish; light transport model

1. Introduction

Improving the performance of modern scintillator-based gamma-ray detectors is fundamental for improving scintillation detector timing resolution for time-of-flight (TOF) positron emission tomography (PET). Many factors, such as the scintillator's intrinsic properties, its optical properties, and the photodetector characteristics, affect the overall system performance (energy, spatial and timing resolution). The light transport in the scintillator and the light collection by the photodetector have a central role, and understanding to optimize them is thus critical for achieving high performance.

In this context, optical Monte Carlo simulations that enable light modeling in the scintillator have been widely used to investigate PET performance[1], given that optical models are available in the widely distributed opensource software Geant4[2] and GATE[3]. Optical simulations were mainly based on the UNIFIED model[4,5], which suffers from major limitations that make anything other than perfectly polished crystals impossible to be simulated with reasonable accuracy[6,7]. Geant4 also included a more realistic model of crystal optical properties developed by Janecek and Moses, whose limitation lies in the complex experimental characterization needed to study crystal surface optical properties[6,8]. Moreover, in their Geant4 implementation, the reflection probability is fixed as a value defined by the user instead of being extracted from the reflectance data.

To overcome these limitations, we previously developed a more customized approach that allows for the computation of the reflectance properties of a given crystal finish using its topography. The algorithm computes the reflectance, transmittance, and photon angular distributions as a function of the incidence angle on the optical interface, composed of the 3D crystal surface attached to a coupling medium[7] (e.g., air or grease). Polished and rough

lutetium oxyorthosilicate (LSO) surfaces (90 μm x 90 μm) were scanned with atomic force microscopy (AFM). The reflectance properties were then saved in a look-up-table (LUT) and used inside a custom optical Monte Carlo simulation to investigate the light transport and the light collection of LSO crystals. In this initial model, the reflectance LUT did not include the presence of a reflector, which was instead processed in a second step inside a customize Monte Carlo code[7]. Excellent agreement with the experimental characterization of crystal light output in select detector configurations, such as with bare crystals or crystal wrapped with a purely Lambertian air-coupled reflector, was demonstrated together with very good agreement with the results of Janecek and Moses[6].

Since scintillators are generally encapsulated in a reflector, the algorithm was then extended to include it within the LUTs computation and was validated in GEANT4 and GATE[9,10]. LUTs for rough and polished LSO crystals coupled to a Lambertian (e.g., Teflon tape) or to a specular reflector (e.g., ESR) using air or optical grease were computed[10]. The light output was evaluated using these crystal-reflector LUTs in the custom Monte Carlo framework and was also measured experimentally for all these combinations at several irradiation depths (from 2 mm to 18 mm from the photodetector face). For all reflector and surface finish combinations, the measured and simulated relative light output showed good agreement, demonstrating the algorithm's capability of accurately modeling the reflections on the crystal's sides[9]. However, the comparison of the measured and simulated light output at the depth closest to the photodetector showed an overestimation of the light output simulated with a rough surface attached to either Teflon and ESR with an air layer. The effect was consistent across depths and was partially explained by a strong effect of the coupling efficiency close to the photodetector face[9], which introduces a constant offset between the configurations.

The work presented here aims at elucidating this behavior through the optimization of the LUT algorithm. We introduce several new features that allow for a more accurate estimation of the reflectance as well as the reflected photon distribution, mainly in the case of rough surfaces.

However, as will be shown further in this article, optical Monte Carlo simulations carried out with these newly generated LUTs, still overestimate the light output. Previous observations suggested that the light output could be strongly affected by a suboptimal coupling[9]. When the reflector is considered to be perfectly coupled to the crystal, and the crystal is modeled as perfectly coupled to the photodetector (ideal simulation), an important overestimation of the experimental light output is observed. In practice, several factors could degrade the coupling, such as a misalignment of the reflector with crystal edges or a non-homogeneous coupling medium.

In this work, air and grease are combined to create *mixed LUTs* with a varying ratio in the mixture to characterize these situations. For example, to simulate the case of grease coupling containing air bubbles, one can imagine a coupling mostly made of grease with a small fraction of air. Alternatively, when considering a reflector air-coupled to the lateral faces of a crystal, the mixed LUT allows modeling some contamination of the interface by a small

amount of optical grease pushed away from the photodetector-crystal face. This interface is no longer an ideal crystal-air coupling.

To study the effect of an imperfect optical coupling of the crystal to the photodetector, which includes the coupling medium close to the photodetector face on the sides, several crystal–coupling–reflector arrangements are simulated using these mixed LUTs. These configurations include a small amount of optical grease pushed from the crystal-photodetector interface to the sides of the crystal, a small grease gap between the reflector and the edge of the crystal due to a misalignment of the reflector with crystal edges close to the photodetector, and the presence of inhomogeneities (e.g., air bubbles) in the crystal-photodetector optical grease coupling. Optical Monte Carlo simulations using these mixed LUTs were performed and compared against experimental data to investigate how these suboptimal optical experimental configurations could lead to a loss of light collection.

2. Materials and Methods

First, the LUT Davis algorithm to compute scintillator-coupling LUTs and reflectors LUTs is described in subsection 2.1, highlighting the changes made from the original code[7,9]. Then, the new mixed LUTs are presented in subsection 2.2. Finally, the coincidence setup and the optical Monte Carlo simulations performed are described in subsection 2.3.

2.1. The optimized Davis LUT algorithm to compute scintillator-coupling LUTs and reflector LUTs

The main change from the original LUTs algorithm structure is the division of the computation in two separate steps (Figure 1(a)). Smaller changes in the algorithm are described in the next subsections. First, given a crystal (defined by its scanned surface, emission spectrum, and index of refraction as a function of the wavelength n_i) and a coupling medium (defined by its index of refraction n_t)), the *scintillator-coupling* reflectance and transmittance LUTs are computed and saved. More details about the scintillator-coupling LUT are given in subsubsection 2.1.1. Second, the transmitted photon information stored in the transmittance LUT is used to compute the reflectance from the reflector (defined by its reflectance and reflected photon angular distribution) and generate the scintillator-coupling-reflector LUT (named *reflector LUT*). More details about the reflector LUT are given in subsubsection 2.1.2.

In the original algorithm, a complete scintillator-coupling-reflector computation was needed when considering a new reflector. With the new two-step structure, the *scintillator-coupling* and the *scintillator-coupling-reflector* computations are carried out independently. Although this new approach increases the number of computational steps, it allows to compute several reflector LUTs from the same scintillator-coupling LUT, thus drastically reducing the computational time when multiple reflectors are tested with the same surface finish and coupling medium.

2.1.1. The scintillator-coupling LUTs—The first part of the LUT algorithm allows computing the scintillator-coupling LUTs. The computation utilizes a microscopic characterization of the crystal surface (e.g., with AFM, confocal microscopy, or 3D

profilometer). A detailed description of the 3×3×20 mm^3 LSO crystal surfaces used in this work can be found in our previous work[7,9]. An example of a 90×90 μm^2 rough scanned surface is shown in Figure 1(b), showing height variations of ~ 6 μm.

To simulate the optical photons emitted isotropically after a gamma interaction and to compute the crystal reflectance and the direction of the photons, the 3D surface is virtually illuminated with a collimated beam of ~2000 photons per angle, each with a specific wavelength randomly extracted by the emission spectrum of the selected crystal, Figure 1(c). The collimated beam impinges the surface with an incident polar angle θ varying between 0° and 90° with an angular sampling of 1°. The beam is also rotated around the global normal to the surface (azimuthal angle ϕ varying from 0° to 360° every 3°) for each polar angle to ensure sufficient sampling of the surface local slope.

Each photon is tracked down to the surface using a new convergence method. The photon's probability to be reflected or refracted by the surface at a specific incident angle is evaluated using Fresnel equations with respect to the local surface normal vector. The local normal vector was previously defined using the four points on the surface closest to the incident point. It is now defined as the normalized sum of four normal vectors, each representing the normal of one of the four triangular surfaces obtained from four adjacent local points. This allows for a better norm definition in the case of highly rough surfaces, where four adjacent points can be strongly non-planar because of the rapid variation of the local surface slope, without increasing the computational time. The Fresnel equations depend on the refractive index of the crystal and of the coupling medium. The index of refraction of LSO is set at 1.82 at all wavelengths. The coupling medium is considered to be air (n=1, LSO-air LUT) for crystal without reflector or optical grease (n=1.5, LSO-grease LUT) for the face in contact with the photodetector entrance window. These scintillator-coupling LUTs are then used to generate the reflector LUT in the case of the scintillator wrapped with, for example, Teflon tape or ESR, as will be described below.

During the LUTs computation, all photons are tested for multiple reflections and/or transmission on the crystal surface, as schematically summarized in Figure 2(a). Multiple transmissions were added to the new code. Reflected photons (*Rcrys)* are ultimately reflected back in the crystal and include directly reflected photons (*Rcrys1*), photons reflected after one or multiple crystal reflections (*Rcrys2)* or photons reflected after a crystal-coupling refraction followed by a coupling-crystal refraction and eventually one or more crystal reflections/refractions (*Rcrys3*). The directly transmitted photon (*Tcrys1),* the ones transmitted after one or multiple crystal reflections (*Tcrys2),* or the ones transmitted after a crystal-coupling refraction followed by a coupling-crystal reflection (*Tcrys3)* are considered as transmitted photons (*Tcrys)*. The crystal reflectance and transmittance are computed as the fraction of photons that are ultimately reflected/transmitted. For a given surface-coupling combination, two LUTs are saved: the crystal reflectance and the transmittance LUT. Together with the reflectance/transmittance and the angular distribution of reflected/transmitted photons as a function of incidence angle, the new LUT now also includes the photon path traveled between the initial incident point and the last interaction point on the crystal surface before an ultimate reflection/transmission. This path is defined by the Euclidean distance and the polar angle (Figure 2(a)).

2.1.2. The reflector LUTs—The second part of the LUT algorithm allows computing reflector LUTs.

The information stored in the transmittance *scintillator-coupling LUT* is used as an input to model a reflector (Figure 2(b)).

The reflector is modeled as a horizontal plane at a distance t from the mean elevation of the surface from its zero plane, defining the coupling thickness as shown in Figure 2(b). As the scintillator surface is not planar, the coupling thickness varies but must be greater than the minimum thickness t_{min}, defined as the distance between the surface mean elevation and minimum elevation. Each transmitted photon is tracked down to the reflector surface. It can be reflected back and forth between the reflector and the crystal, with an angular distribution determined by the reflector and crystal characteristics, Figure 1(c-d). Once back in the crystal, it can be eventually reflected/refracted multiple times by the surface. The photon can face a maximum number of 1000 internal reflections within the coupling, after which it is considered as transmitted. Although included in the model, the coupling absorption is considered to be zero in this work.

The optimized algorithm allows simulating thicker coupling medium thicknesses more accurately. The scanned surface has a limited dimension (e.g., 90×90 μm^2), which means photons can travel distances greater than the surface dimension within the coupling, such as in the case of multiple reflections within the surface-reflector interface or reflections with a high angle on the reflector. These are non-negligible situations even with a relatively thin coupling thickness, which becomes even more frequent with thicker coupling media where the photons travel more between each interaction. Consequently, in the optimized algorithm, a larger surface is formed by concatenating surfaces vertically and horizontally flipping the scanned surface. A photon can travel within the coupling a distance of a maximum of 50 times the scanned surface dimension (e.g., 4.5 mm).

Ultimately, a photon can be refracted again inside the crystal, contributing to the reflectance LUT or can definitely cross the reflector and be transmitted (*Rref* and *Tref*, respectively Figure 2(b)), contributing to the transmittance LUT.

For a given surface-coupling-reflector combination, the reflectance and transmittance LUTs are saved. Each contains the reflectance/transmittance, the angular distribution of reflected/transmitted photon, and the traveled distance in the coupling medium as a function of the incident angle. The ultimate reflectance and angular distribution of the reflected photons are a combination of photons reflected by the crystal *Rcrys* and photons reflected by the reflector that ultimately re-enter the crystal *Rref*. The transmittance and angular distribution of transmitted photons are the combinations of all photons *Tref* ultimately transmitted as discussed in subsection 3.1.1.

In this work, we model a specular reflector (ESR, 3M) and a Lambertian reflector (Teflon tape with 4 layers of wrapping), based on our previous work[9]. Two coupling media between the reflectors and the crystal modeled air (n=1) or optical grease (n=1.5), so two scintillator-coupling LUTs were used as input to calculate the reflector LUTs: LSO-air or LSO-grease.

Most optical simulations that will be presented were performed with a thickness of 10 μm, representative of a common reflector attached by a manufacturer[11]. However, we also studied the photon traveled distance for a thicker coupling of 100 μm, representative of some reflective tapes that are also applied on scintillators (100 to 200 μm). The reflectance and transmittance, together with the angular distributions and the traveled distance of reflected and transmitted rays obtained with the optimized code, are shown in the results section 3.1.

2.2. Simulating suboptimal optical configuration: the Mixed LUTs

The mixed LUTs, introduced with the new algorithm, are a combination of two existing scintillator-coupling LUTs or reflector LUTs (e.g., LSO-air and LSO-grease LUTs or LSO-air-ESR and LSO-grease-ESR LUTs). They are generated by randomly selecting the optical photon fate through reflectance, angular distribution, and traveled distance according to their ratio in the mixture, for each polar angle θ and at each azimuthal angle ϕ. Given the high statistics used to generate the existing LUTs, this approach allows the generation of reliable mixed LUTs within a few minutes without the need for running a complete LUT computation. We validated this method by carrying out a complete simulation of a mixture composed of 50% air and 50% grease, tracking down each photon to the interface with the coupling. As the coupling can be air or grease, its index of refraction was randomly changed accordingly to the relative fraction grease-air.

Since the actual relative fractions of air in grease and vice-versa are unknown, we performed a sensitivity study by sampling the air-grease ratio every 10% from 10% to 90% and generating the corresponding LUTs. The study was carried out for both ESR and Teflon coupled to a polished and rough surface. The reflectance and transmittance together with the angular distributions of reflected and transmitted rays obtained with the mixed LUTs are shown in the results section 3.2.

Although not considering spatial variations of the coupling, this mixture model can describe medium inhomogeneities to make optical Monte Carlo simulations more realistic and representative of an experimental setup. A comprehensive description of all the simulated configurations is further done in subsection 2.3.2.

2.3. Simulation configurations

2.3.1. Photon tracking Monte Carlo code—In this work, we used a custom optical Monte Carlo code to simulate the light output of the LSO crystals, which were previously characterized experimentally without reflector, or wrapped in ESR and Teflon tape[7,9,10].

We used this customized Monte Carlo code with $3\times3\times20$ mm^3 rough LSO crystals matching the experimental setup described in section 2.4: light yield of 35 photons/keV, absorption length of 800 mm, refractive index of 1.82 for all wavelengths, decay time of 40 ns, and a rise time of 72 ps. All photons crossing the scintillator-coupling medium toward the photodetector were considered detected (geometrical efficiency of 1 and quantum of efficiency of 1). For all configurations, a total of 200 gamma interactions was simulated 2 mm from the photodetector face, with a depth bin of 2.5 mm. Each photon was assigned

an emission time and wavelength sampled from the scintillator decay time distribution and emission spectrum, respectively.

Several crystal-photodetector-reflector arrangements were simulated using different LUTs at the crystal borders and are described in next subsubsection.

The number of detected photons per event at a 2 mm irradiation depth was recorded as light output in all simulations. All light output values were then normalized by that of the bare crystals in contact with air. Only relative changes in light output were considered to compare experiments and simulations, as absolute quantification of the number of collected photons was not available experimentally (the LSO light yield, the photodetector quantum efficiency, and SiPM gain are not accurately known).

2.3.2. Optical simulations—All simulated configurations are summarized in Table 1. A schematic view is also shown in Figure 3. All optical simulations were performed with a thickness of 10 μm. First, the Monte Carlo code was used to validate the new LUT algorithm with ideal crystal-photodetector and crystal-reflector couplings (Table 1), as shown in Figure 3(a). The crystal face in contact with the photodetector was modeled as a polished surface perfectly coupled with optical grease. All five rough faces were either coupled to ESR (air or grease coupled), Teflon, or to no reflector. Results are shown in subsection 3.3.1.

To show the effect of medium inhomogeneities, we performed a light output sensitivity study by using mixed air-grease ESR LUTs (every 10% from 0% to 100% of air in the coupling) on the five crystal's sides (configuration 1 in Table 1). The photodetector face was modeled as a polished surface coupled with optical grease. Results are shown in subsection 3.3.2.

Although being useful to understand the impact of mixed LUTs in the optical simulations, this sensitivity study assumed that the air/grease ratio was uniform across a crystal face, while in reality the grease is primarily located close to the photodetector face, where it would have the strongest effect.

To study the effect of a suboptimal optical coupling of the crystal to the photodetector and subsequent imperfect modeling of the coupling medium close to the photodetector face, we used several mixed LUTs with a rough surface finish in several more realistic arrangements, which are schematically depicted in Figure 3(b).

First, a misalignment of the reflector at the crystal edges could cause the presence of a small gap of air or grease between the edge of the reflector material and the edge of the crystal (Figure 3(b)). Since optical grease is commonly used as a coupling material for the photodetector, we assumed this gap to be in contact with optical grease. To do so, we added a grease gap of 0.2 mm, 0.4 mm, 0.6 mm, or 0.8 mm between the crystal edge and the reflector edge close to the photodetector face (configurations 2 in Table 1). Results are shown in subsection 3.3.2.

Second, some fraction of the optical grease used to couple the crystal to the photodetector can get pushed to the sides of the crystal when coupling them. This disrupts the crystal-air

interface in the case of Teflon-air and ESR-air, thus changing the index of refraction of the coupling medium and, subsequently, the efficiency of the reflector. This may decrease the light output and, if not considered in simulations, lead to its overestimation. To model this effect, an infiltration zone was considered close to the photodetector face along the sides of the crystal when air-coupled to the reflector. The thickness of the infiltration area was varied from 0.5 mm to 4 mm starting from the photodetector face (configurations 3 in Table 1). For each thickness value, several degrees of infiltration were tested by using the air-grease mixed LUTs. The rest of the crystal sides were modeled by an LSO-air-reflector LUT. Results are shown in subsection 3.3.3.

Third, we hypothesize that the grease coupling of the crystal to the photodetector could be inhomogeneous, containing air bubbles, thus reducing the light output. The presence of a small amount of air in the crystal-photodetector optical grease coupling was tested by using two mixed LUT with no reflector, with 5% and 10% of air in the coupling medium (configuration 4 in Table 1). On the four lateral sides, we used Teflon and ESR (air-coupled or grease-coupled). Results are shown in subsection 3.3.4.

Then, we studied the simultaneous effect of these three suboptimal optical couplings. First, we added a grease gap and small regions of the crystal-reflector coupling with grease infiltration, maintaining a perfect crystal to photodetector coupling (configuration 5 in Table 1). Second, we added air inhomogeneities in the photodetector coupling (configuration 6 in Table 1). Results are shown in subsection 3.3.5.

Lastly, it is known that Teflon reflectance can deteriorate over time because of grease absorption due to the Teflon permeability, which could have a strong effect on the detected light output. To account for it, we artificially decreased Teflon reflectivity by 0.95% and 0.9%. Results are shown in subsection 3.3.6. ESR, being less permeable, is probably not affected by the presence of optical grease. Thus, these effects are expected to have a minimum impact in the case of ESR, even more when coupled with grease, in which optical grease is already present at the crystal-photodetector border.

2.4. Validation against coincidence measurements

The LUT computation was validated against experimental data using two rough 3×3×20 mm^3 (LSO) crystals, which 3D surfaces served for the LUT generation. Each crystal had five rough faces and one polished face coupled to the photodetector. All samples were coupled to a silicon photomultiplier (SiPM, RGB-HD, FBK) using optical grease (Bicron BC-630). The samples were tested with and without the reflector. ESR (both air-coupled and grease-coupled) and Teflon wrapped in 4 layers were used.

The coincidence setup is described in detail in[9,12]. Briefly, the detector of interest was placed in coincidence with a reference detector (3×3×5 mm^3 LFS reference crystal coupled to another SiPM RGB-HD, FBK). Both detectors were irradiated with a ^{22}Na point source at 2 mm from the photodetector face. The irradiation beam was estimated to be ~2.5 mm wide (accounting for the source-detectors distances and the point source diameter). Each configuration was characterized in terms of light output at the irradiation depth, defined as the 511 keV photopeak position.

3. Results

3.1. Optimized LUT Davis Model

The effect of the new features implemented in the optimized algorithm (multiple reflections, photon path in the coupling medium, reflector LUT) is described in the following two subsections.

3.1.1. Effect of multiple reflections on the scintillator-coupling LUTs—

Figure 4 shows the angular distribution of reflectance for the polished and rough crystals in contact with air and grease, including all photons *Rcrys*. The sum of the reflectance and transmittance naturally equals 1 in the absence of absorption.

For the polished surface coupled with air or grease (Figure 4(a)), a good agreement between the reflectance of the optimized and the original code is obtained. This indicates that the improved modeling of multiple reflections only minimally affects the polished surface LUTs. This is due to the fact that most reflected photons *Rcrys* undergo a single reflection due to the surface smoothness, as shown by the overlap between *Rcrys* and *Rcrys1* in Figure 4(a).

In contrast, the code optimization (new convergence method for the incident point, new normal vector definition, presence of multiple reflections, and transmission) changed the reflectance of the rough surface, as shown by the discrepancies with the original code (blue and red solid curves in Figure 4(b-c)). With the rough surface, the contribution of multiple reflections and refractions is non-negligible for both coupling media, as shown by the differences between the individual contributions of the reflected photons depending on the number of reflections (*Rcrys1, Rcrys2,* and *Rcrys3*). While in contact with air, reflections were preferred to transmissions (critical angle of 33° for the LSO-air interface). In particular, direct reflections *Rcrys1* were predominant at all incident angles (Figure 4(b)). Reflections after one or multiple reflections *Rcrys2* were preferred to reflection after one or multiple transmissions *Rcrys3* at all angles, although the difference decreased at high incidence angles due to an increasing shadowing effect[7]. It is already known that the average surface slope seen by photons with an incidence angle greater than 60° increases[7]. This, in turn, increases the photon probability of undergoing multiple refractions between surface peaks and consequently the probability of collecting photons reflected after multiple transmissions. In contrast, opposite trends were observed with a grease coupling (Figure 4(c)). The majority of the events were transmitted at the crystal-coupling medium interface due to a higher critical angle of 55° for the LSO-grease interface, as shown by a lower *Rcrys* compared to the crystal-air coupling shown in Figure 4(b). The reflected events were mainly directly reflected (*Rcrys1*). More reflected photons had undergone some transmission instead of multiple reflections only: *Rcrys3* was greater than *Rcrys2*, opposite to the air coupling. With both air and grease, grazing incidence close to 90° strongly favored direct reflection *Rcrys1* (Figure 4(b) and Figure 4(c)). This can be explained by the fact that when an incident photon arrives on the surface at grazing incidence, it cannot reach valleys and thus only interacts with high-elevation surface peaks. When interacting with a medium-slope high peak (a surface “hill”), the local angle is almost always larger than the critical angle, thus reducing the transmission (and consequently *Rcrys3*) in favor of direct

reflection *Rcrys1*. Although not shown, with the rough surface the majority of transmitted photons are directly transmitted for both coupling media.

The optimized LUT code changes the angular distribution of reflected and transmitted photons from those obtained with the original code[8]. However, its effect is greater with a rough surface, but the diffuse nature of the surface and the angular distribution makes it more challenging to visualize these changes.

3.1.2. Reflector LUT—The reflectance and transmittance of ESR and Teflon obtained with the optimized algorithm are similar to the one shown in our previous work[9]. The photons finally reflected are photons directly reflected from the crystal and that directly refracted from the coupling-scintillator surface, as expected with an optical interface from lower to higher index of refraction (not shown).

The Teflon and ESR reflectance curves were very close. However, the angular distribution of the reflected photons for two materials greatly varied since ESR is a specular reflector and Teflon is a diffuse reflector. The Lambertian nature of Teflon spreads the direction of reflected photons over a spherical cap with an angle of 33° when air-coupled and 55° when grease-coupled, corresponding to the critical angles between LSO and air or grease, respectively[9].

3.1.3. Photon path in the crystal-reflector coupling—Figure 5 shows the photon path in a 10 μm- or 100 μm-thick coupling interface filled with grease for a rough surface coupled to ESR. Results are shown at incidences 10° and 40°. As expected, the thinner the coupling, the shorter the total path since a photon traveled to a shorter distance between interactions with the surface. With a thickness of 10 μm and an incident angle of 10°, the most frequent distance was 3.6 μm (Figure 5(a)), much shorter than the 40 μm distance observed with a 100 μm interface (Figure 5(b)). When increasing the incident angle to 40°, the crystal-coupling refraction angles increased and, consequently, the reflection angles by the specular reflector (ESR) increased. Photons reflected at grazing incidence more frequently therefore traveled a longer distance in the coupling medium: 19 μm and 185 μm at the peak for the 10 μm and 100 μm thicknesses, respectively. These considerations are also supported by the tails of the distributions shown in Figure 5(c) and Figure 5(d). With 10 μm, less than 0.02% of the photons traveled more than 500 μm with a maximum of 1.8 mm, for both 10° and 40°. With 100 μm, 2% of the photons traveled more than 500 μm with a maximum of 2.2 mm.

It is important to note that for both incident angles shown in Figure 5, a fraction of photons traveled a longer distance than the scanned surface length of 90 μm inside the coupling (0.3% and 0.6% with 10 μm and 5% and 99% with 100 μm, both at 10° and 40°, respectively). This implies that the algorithm needs to track photons over a larger distance, which can be achieved by stitching together several surface samples as described in subsubsection 2.1.2. This, however, strongly increases the computational time.

All light output results presented in the next sections were obtained with a crystal-coupling interface of 10 μm. Thus, the effect of the traveled distance is considered negligible and

was not included in the custom Monte Carlo simulation code. Nevertheless, 2% of photons travel more than 500 μm with a 100 μm grease coupling and an angle of 40°. Considering the crystal dimension ($3\times3\times20$ mm^3), we can conclude that these photons could affect the detected light output if thicker coupling media are used, mainly due to photon loss close to the photodetector face.

3.2. Reflectance and transmittance of a Mixed coupling medium

Reflectance and transmittance curves of various air-grease mixtures without reflector described in section 2.2 are shown in Figure 6. The envelope is defined by 0% and 100% air, similar to Figure 4.

Figure 6(a-b) shows that with the polished surface, the composition of the mixture primarily affected photons which incidence angle is between the critical angles (33°−55°). In this range, reflections were favored when the fraction of air was greater (red and dark orange shades in Figure 6(a) for reflection; cerulean to dark blue shades in Figure 6(b) for the correspondent transmission). When progressively adding grease in the air coupling, the reflectance decreases (from orange to yellow) and eventually becomes lower than the transmittance (from light blue to green) when there is more grease than air. A similar pattern is observed with the rough surface in Figure 6(c), although the reflectance is altered over the entire angular range. The same trend with less amplitude is visible in the reflectance of the polished and rough surface coupled with ESR, shown in Figure 6(d) and Figure 6(e), respectively.

These results indicate that the contamination of either an air interface with grease or a grease interface with air (e.g., bubbles) will change the reflection pattern in the crystal and thus the amount of detected light in the optical Monte Carlo computation, as further shown in the results.

3.3. Light output

The maximum light output obtained for all the configurations described in Table 1 is shown in this section.

3.3.1. Ideal couplings—First, the Monte Carlo code was used to validate the new LUT algorithm with ideal crystal-photodetector and crystal-reflector couplings (Figure 3(a)).

Figure 7 shows the light output results obtained for the rough surface with no reflector, Teflon, ESR air-coupled or grease-coupled (in Table 1). All values were normalized by the light output of the rough crystals with no reflector.

Overestimations of 31%, 22% and 3% were obtained when comparing the simulated light output of Teflon, ESR air-coupled or grease-coupled to their experimental values. As a comparison, the original code yielded overestimations of 39%, 25% and 14%[9], showing that the optimization of the algorithm only moderately improved the accuracy of the simulated light output and that further inaccuracies remain. The relative light output as a function of the irradiation depth remained in good agreement with the experimental curves, similar to our previous work[9].

The next configurations investigate whether a more realistic contact between the crystal and the reflector and the crystal and the photodetector than that assumed here, could explain the lower experimental light output (Figure 3).

The light output was computed for various non-optimal Teflon or ESR optical coupling by using the air-grease *mixed LUTs* in several geometrical arrangements with a rough surface finish (Table 1).

3.3.2. Effect of the crystal border coupling—The effect of medium inhomogeneities was studied by performing a light output sensitivity study using mixed air-grease ESR LUTs (every 10% from 0% to 100% of air in the coupling) on the five crystal sides (configuration 1 Table 1). Figure 8(a) shows the light output as a function of the air /grease ratio in the coupling medium between the rough surface and ESR (light blue). Experimental results (yellow) and the ideal simulation light output (blue) are shown as a reference. Gradually decreasing the amount of air by adding grease in the crystal-air-reflector border resulted in a gradual decrease of the light output from the ideal simulation with 100% of air (i.e., 0% grease) (blue bar, left). It can be explained by a decrease of the overall reflection efficiency over the crystal-reflector assembly. The light output obtained using the mixed LUT (50% air) matches the full computation using a 50% air-50% grease LUT (green bar on the right) with an error <1%, thus validating the mixed LUT computation procedure.

These results show the strong impact of the presence of impurities in the coupling medium when conducting optical simulations with the LUT Davis model. This study assumes that the air/grease ratio is uniform across a crystal face, which is probably unrealistic as the grease is primarily located close to the photodetector face. To study the effect of more realistic suboptimal optical coupling of the crystal to the photodetector and of the imperfect modeling of the coupling medium close to the photodetector face, we studied several crystal-reflector-photodetector arrangements.

First, we simulated the reflector's misalignment at the crystal edges by adding small grease gaps (0.2 mm, 0.4 mm, 0.6 mm, or 0.8 mm) between the edge of the reflector material and the edge of the crystal (configurations 2 in Table 1, Figure 3(b)).

For all arrangements, the presence of a grease gap along the crystal side locally reduced the reflectance close to the photodetector face (Figure 8(b)). With a crystal cross-section of 3×3 mm^2 and a depth-of-interaction of 2 mm from the photodetector face, the photons arrive on the gap with an angular distribution that favors transmission over reflection, which means that more photons will be subjected to the locally decreased reflectivity. This results in a loss of photons reaching the photodetector for a given gamma event, hence a lower light output.

The same relative light output decrease is obtained when considering Teflon and ESR-air. The light loss reached 10–12% for a grease gap of only 0.2 mm (e.g., 1/100 of the detector thickness when considering 20 mm-long crystals), indicating a strong effect of coupling impurities or geometrical defects. Light output values comparable to the experimental values were observed with a gap of 0.8 mm and 0.6 mm, for Teflon and ESR-air, respectively.

When considering a grease coupling (ESR-grease), adding a 0.2 mm gap produced a light output comparable to the experimental value, a much larger decrease than for the air coupling with the same gap (Figure 8(b)). This suggests that the presence of a grease gap is the primary cause of light loss in the ESR-grease configuration. The small 2% difference points to a slightly bigger gap (~0.225 mm extrapolated from the linear interpolation of the light output as a function of the gap length), a non-uniform gap over the 3×3 mm^2 crystal cross-section, or a second-order effect such as the presence of inhomogeneities in the photodetector coupling, as will be discussed further in the results.

The greater effect of a grease interstice when using an air-coupled reflector suggests that the index of refraction mismatch between the grease gap and the crystal-reflector coupling plays an important role in the light output. We will further study the combined effect of the gap and small regions of grease infiltration in the crystal-reflector coupling. Since no experimental evidence is available due to the difficulty to measure those effects, these results can only be qualitatively interpreted to explain the light output decrease but highlight the need for excellent alignment of the crystal and reflectors in experimental setups.

In the rest of this work, we will only consider a 0.2 mm gap that showed good agreement with ESR experimental results and is consistent with previous microscopic observations of manually wrapped crystal[9].

3.3.3. Effect of grease infiltrated within the crystal-reflector interface—A generous amount of optical grease or glue used to couple the photodetector to the crystal can lead to some coupling pushed into the crystal-reflector air interface close to the photodetector face. Infiltration zones with lengths varying from 0.5 mm to 4 mm from the photodetector face, with different degrees of grease infiltration, were modeled through the air-grease mixed LUTs (Configurations 3, Table 1). The LSO-air-reflector LUT was used on the rest of the crystal sides.

The resulting light output are shown in Figure 9 for Teflon and ESR-air (green shades) and compared to the experimental light output (yellow bar) and the ideal simulation (blue bar). For a given infiltration thickness, increasing the amount of grease in the mixture decreased the light output due to the reduced crystal-reflector reflectance close to the photodetector face. For the same reason, the light output decreased as a function of the infiltration thickness for a given amount of air in the mixture. A relative light output decrease of 2% was obtained for both ESR and Teflon from 100% of air to 0% of air (100% of grease) in a 0.5 mm-thick infiltration zone. The relative decrease goes up to 11% and 15% for Teflon and ESR, respectively, when considering a 4 mm-thick infiltration, which is relatively large considering a 20 mm-thick crystal.

However, comparing the results with the experimental value, none of these suboptimal optical configurations alone can fully justify the simulated light output overestimation. Consequently, the effect of grease infiltration will be studied in conjunction with other effects in the Results subsubsection 3.3.5.

3.3.4. Effect of air in the crystal-photodetector coupling—The light output obtained while simulating the presence of a small amount of air (5% and 10%) in the crystal-photodetector optical grease coupling is shown in Figure 10 (dark and light orange, respectively), together with the experimental results (yellow) and the ideal simulations (blue).

For both Teflon-air and ESR-air, a 5% amount of air decreased the light output by 2% and 4%, respectively. The decrease rose to 3%, 4%, and 7% in the case of 10% of air in the coupling for Teflon and ESR coupled with air and grease, respectively.

When considering the ESR-grease configuration, the effect of a 5% air non-homogeneity leads to an underestimation of the experimental light output. This suggests that the fraction of air non-homogeneities could be lower than 5% if considered as the only suboptimal optical effect on light output. A linear interpolation of the light output as a function of the fraction of air in the coupling points to an estimation of 1.8% air producing a light output comparable to the experimental value. However, this value will be lower when combining the effect of air in the crystal-photodetector coupling and a small grease gap (subsection 3.3.2).

The actual amount of air in an experimental optical grease coupling cannot be easily quantified and is likely to vary strongly from one experimental setup to another. These results provide a qualitative evaluation of the effect of non-homogeneities in the crystal-photodetector coupling, accessing individual parameters that cannot be characterized experimentally.

3.3.5. Combined effect of grease gap, inhomogeneities in the crystal-photodetector coupling and grease infiltration—After studying the individual effect of these three factors, we investigated their combined effect. Figure 11 shows the light output results obtained for ESR-air and Teflon with several combinations: a 0.2 mm grease gap all around the photodetector face, three infiltration zones thicknesses (0.5, 2.5 and 4 mm) with different degree of infiltration (0%, 40%, and 100%), and a photodetector-crystal interface only composed of grease (configurations 5 Table 1).

As already discussed in subsubsection 3.3.2, the presence of a small grease gap of 0.2 mm between the crystal and the reflector (light blue bars) decreased the light output by 10% −12% compared to the ideal coupling, shown in royal blue on the left. When considering the presence of this gap together with a 0.5 mm infiltration zone starting at the crystal-photodetector interface, the light output did not decrease with the fraction of air present in the mixture for either Teflon or ESR-air (dark blue bars). These results suggest the presence of a thicker infiltration zone.

For the ESR-air (Figure 11(a)), Increasing the infiltration zone length decreased the light output by 24% compared with the ideal simulation results (blue bar) and the 2.5 mm infiltration zone and 0% of air in the mixture (Figure 11(a), last green bar on the right). This configuration produced a light output comparable to the experiments (<1% difference), suggesting how a small amount of air (less than 1%) in the photodetector interface could

degrade the light collection and may be modeled in the simulations for a good agreement with experiments. In fact, modeling a thicker infiltration zone with a higher amount of air in the mixture (and of air in the photodetector coupling) could lead to a stronger agreement with the experiments (Figure 11(a)).

In the case of Teflon, even when considering both effects in the worst scenario (thickest infiltration zone (4 mm) and 0% of air in the mixture, last red bars on the right), the simulation still overestimated (+15%) the experimental light output. No simulation configuration matched the experimental light output with Teflon.

3.3.6. Effect of Teflon reflectivity—The optical grease entering the crystal-reflector coupling likely gets partially absorbed by the Teflon tape, deteriorating its reflectivity. Practically, this can be observed by discoloration of the Teflon itself[9].

Figure 11(c) shows the light output obtained by manually decreasing the Teflon reflectivity from 0.95% to 0.9% for a 0.5 mm and a 2.5 mm infiltration zones without air in the mixture (100% grease). The results show how the large light loss could be due to a small infiltration zone (0.5 mm) characterized by a reflectance of more than 90% or by a thicker infiltration zone characterized by a reflectance efficiency decreased of 95% and 90%.

4. Discussion

In this work, we presented an optimized computation of the reflectance and transmittance LUTs for the LUTDavis model we previously developed for optical Monte Carlo simulation with GATE[7,9,10]. The LUTs contain the reflectance probability and the reflected photon angular distribution as a function of the incidence angle.

The algorithm allows for an accurate definition of the reflectance of a surface without and with reflector with a variety of coupling media. After the generation of the LUT without reflector (scintillator-coupling LUT), the optimized algorithm uses these LUTs to compute the effect of a reflector. That allows performing the simulation of several reflectors from the same scintillator-coupling LUT, leading to an important computational time gain when multiple configurations of the same surface are needed for detector optimization.

The reflector is considered as a flat surface since no information about reflectors shape once coupled to the crystal is available. Preliminary studies of the distance traveled by photons inside the coupling medium show the need to include this parameter in optical Monte Carlo simulations when thick crystal-reflector couplings are of interest, as in the case of reflective tapes (100 to 200 μm). Indeed, increasing the thickness of the crystal-reflector coupling to values representative of such an experimental situation can increase the traveled distance in the coupling up to a few mm (Figure 5). These events lead to light loss close to the photodetector face, especially when the photodetector sensitive area dimension is comparable to the crystal exit face surface. This will be included in further future investigations. Although thick couplings can be modeled, in this case the need for a larger surface sample to account for long traveled distances in the coupling extends the computational time.

The LUT model now gives the possibility to generate LUTs with a mixture of coupling media, with and without reflector. These new LUTs model suboptimal optical couplings between the crystal and the photodetector as well as imperfections of the crystal-reflector coupling, which should be studied to better understand the possible sources of light loss experimentally measured.

Our results present a detailed characterization of the effect of crystal-reflector and crystal-photodetector coupling imperfections close to the photodetector face on the extracted light output, when the gamma irradiation point is close to the photodetector face.

The strongest effect is observed with the presence of a small gap of grease. The same relative light output decrease is obtained when considering the same coupling but a different reflector. The greater effect of this gap when considering an air-coupled reflector than a grease-coupled one suggests that the index of refraction mismatch between the grease gap and the crystal-reflector coupling is playing a crucial role in the light output loss. Our simulation study shows how a tiny 0.2 mm gap leads to a 10%−12% light output loss, which increases up to 32% with a 0.8 mm gap. The gap should always be minimized during the experimental crystal wrapping. Microscopic observations of the setup could help researchers understand the impact of this imperfection on their experimental results.

The presence of optical grease infiltrating the crystal-reflector air coupling decrease the light output, and the same infiltration zone dimension has a different effect on the light output when considering different reflectors. This indicates the importance of modeling it during realistic detector simulations for both detectors optimization when considering different surface-coupling-reflector arrangements and results analysis since the majority of experimental detector setups use optical grease to couple the photodetector to the crystal and may suffer from some grease pushed out from the photodetector face to the sides, as shown in Figure 3. The goal of the authors is not to match the simulation and the experimental results but to provide a detailed understanding of the light loss due to such imperfections.

These two effects together could be sufficient to explain the discrepancy of the relative light output obtained with ESR in simulations and experiments. In the case of Teflon, the study indicates that the light output strongly depends on the imperfection of the reflector wrapping, including a deterioration of the reflectance due to the absorption of optical grease by Teflon. Good agreement with the experimental results can be obtained only by accounting for a lower reflectance. ESR, being less permeable, is less affected by the presence of optical grease. Its effect is only apparent on a slightly different reflectance trend as a function of the incident angle. Even causing a weaker effect, air inhomogeneities in the photodetector face could lead to light loss.

Although it is not possible to exactly model all the imperfections in the reflector wrapping and in the photodetector coupling and to control for all experimental laboratory conditions, a high-fidelity model of the inevitable practical limitations can lead to an increased understanding of the experimental results. Having a critical view of different surfaces and reflector behavior used in experimental conditions can ultimately help advance detector optimization.

All these considerations can be made since relative values of light output are considered. While comparing absolute values, the photodetector geometrical and quantum efficiency play a crucial role in detector optimization and need to be included.

5. Conclusion

We presented the optimization of the LUT Davis algorithm. The LUT model is included in GATE since its version v8.0[10]. Until now, users were able to choose one of the two surfaces available (a polished and a rough one) to be used in their specific application. For each surface, four LUTs are available: with no reflector, Teflon, ESR-air and ESR-grease. These available LUTs will be updated in future GATE releases to account for the optimization presented in this work. In future work, the traveled distance in the crystal-reflector coupling will be included in the GATE LUT.

Our results indicate that when comparing the performance of detector with different finishes (reflector or coupling medium), performing simulations in ideal conditions can lead to an overestimation of the light output. Researchers must carefully consider all potential sources of practical limitations to perform an accurate comparison of light output values and ultimately have a reliable detector performance optimization.

The first step towards high-fidelity modeling of a detector lies in the use of highly customized LUTs. In parallel to this work, we developed a standalone application to allow users to generate fully customized GATE LUTs for their own surfaces, setting the intrinsic properties of their scintillators and of the coupling medium of interest and choosing a specific reflector of interest[13]. This application is now available and can be downloaded by GATE users[14].

Acknowledgements

This work was supported in part by NIH grant EB027130. C. Trigila is with the Department of Biomedical Engineering, University of California Davis, Davis, CA 95616, USA. E. Roncali is with the Department of Biomedical Engineering and the Department of Radiology, University of California Davis, Davis, CA 95616, USA.

References

1. Roncali E, Mosleh-Shirazi M.A, Badano A. Modelling the transport of optical photons in scintillation detectors for diagnostic and radiotherapy imaging. Physics in Medicine & Biology, 2017; 62(20): R207. [PubMed: 28976914]
2. Agostinelli S, Allison J, Amako KA, et al.GEANT4—a simulation toolkit. Nuclear instruments and methods in physics research section A: Accelerators, Spectrometers, Detectors and Associated Equipment. 2003; 506(3): 250–303.
3. Jan S, Santin G, Strul D, et al.GATE: a simulation toolkit for PET and SPECT. Physics in Medicine & Biology, 2004; 49(19): 4543. [PubMed: 15552416]
4. Nayar SK, Ikeuchi K, Kanade T. Surface reflection: physical and geometrical perspectives. IEEE Transaction on pattern analysis and machine intelligence. 1991; 13(7): 611–634
5. Levin A, Moisan C. A more physical approach to model the surface treatment of scintillation counters and its implementation into DETECT. IEEE Nuclear Science Symposium. Conference Record. 1996; 2: 702–706
6. Janecek M, Moses WW. Simulating scintillator light collection using measured optical reflectance. IEEE Transactions on Nuclear Science. 2010; 57(3): 964–970.

7. Roncali E, Cherry S. Simulation of light transport in scintillators based on 3D characterization of crystal surfaces. Physics in Medicine & Biology. 2013; 58(7): 2185–2198 [PubMed: 23475145]
8. Janecek M, Moses WW. Measuring light reflectance of BGO crystal surfaces. IEEE Transactions on Nuclear Science. 2009; 55(5): 2443–2449
9. Roncali E, Stockhoff M, Cherry S. An integrated model of scintillator-reflector properties for advanced simulations of optical transport. Physics in Medicine & Biology. 2017; 62(12): 4811 [PubMed: 28398905]
10. Stockhoff M, Jan S, Dubois A, et al.Advanced optical simulation of scintillation detectors in GATE V8. 0: first implementation of a reflectance model based on measured data. Physics in Medicine & Biology. 2017; 62(12): L1. [PubMed: 28452339]
11. Du J, Ariño-Estrada G, Bai X, et al.Performance comparison of dual-ended readout depth-encoding PET detectors based on BGO and LYSO crystals. Physics in Medicine & Biology. 2020
12. Kwon SI, Ferri A, Gola A, et al.Reaching 200 ps timing resolution in a time-of-flight and depth-of-interaction positron emission tomography detector using phosphor-coated crystals and high-density silicon photomultipliers. Journal of Medical Imaging. 2016; 3(4):043501. [PubMed: 27921069]
13. Trigila C, Moghe E, Roncali E. Standalone application to generate custom reflectance Look-Up Table for advanced optical Monte Carlo simulation in GATE/Geant4. Medical Physics. 2021.
14. Roncali lab website. Documentation. https://roncalilab.engineering.ucdavis.edu. AccessedApril 15, 2021.

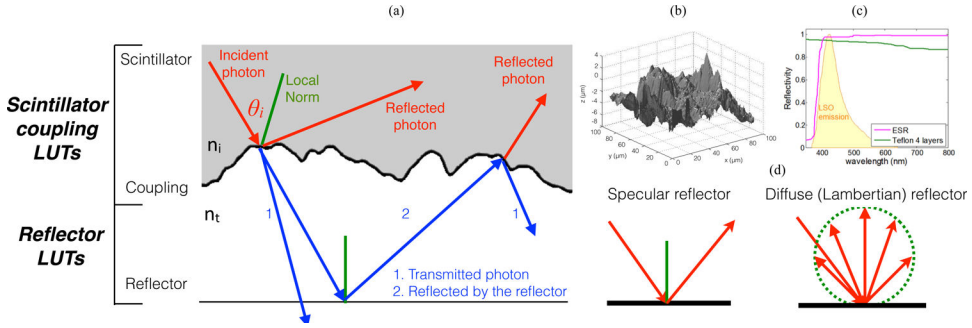

Figure 1.

(a) Schematic view of the Davis LUT algorithm. First, the reflectance and transmittance LUTs for the scintillator-coupling medium interface are computed using a specific surface measurement and the scintillator intrinsic properties. Second, the reflector LUT computation is performed using the reflector reflectivity and specific angular distribution of reflected photons (n_i and n_t represent the scintillator and coupling indexes of refraction, respectively). (b) Example of a rough surface scanned with an AFM. (c) LSO scintillator emission spectrum superimposed with the reflectivity of a Lambertian reflector (Teflon) and a specular reflector (ESR). (d) Angular distribution of photons reflected by a specular or Lambertian reflector.

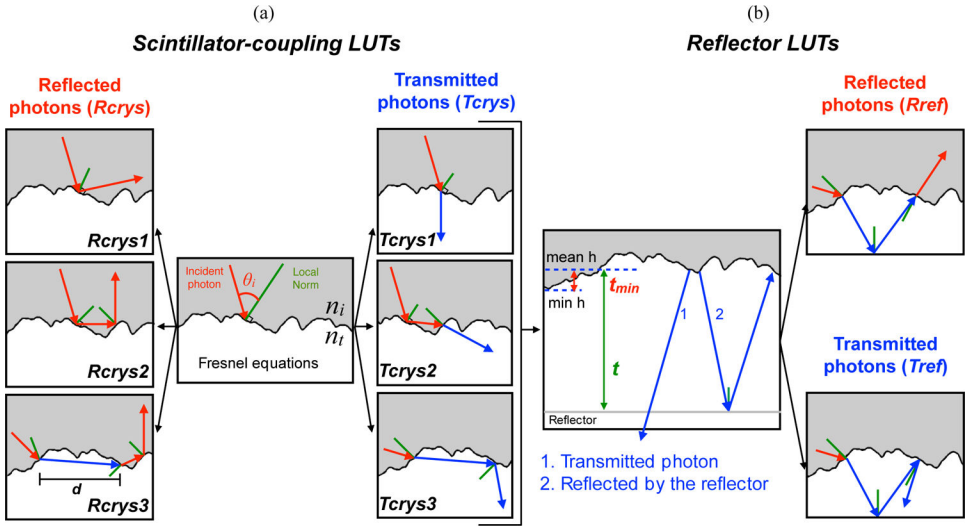

Figure 2.

(a) Schematic processing of an optical photon arriving at the crystal interface with an incident angle θ during the scintillator-coupling LUTs computation. Left: Cases in which a photon is reflected by the scintillator (Rcrys), composed by the sum of the directly reflected photons (Rcrys1), the photons reflected after one or multiple reflections (Rcrys2), and the photons reflected after one or multiple refractions (Rcrys3). d represents the Euclidean distance. Right: Cases in which photons are considered transmitted by the scintillator (Tcrys = Tcrys1+Tcrys2+Tcrys3). (b) Schematic view of the reflector LUTs computation starting from the transmitted photons computed in the scintillator-coupling LUTs. The coupling thickness t is calculated from the mean surface elevation (mean h) and must be greater than the minimum thickness t_{min}.

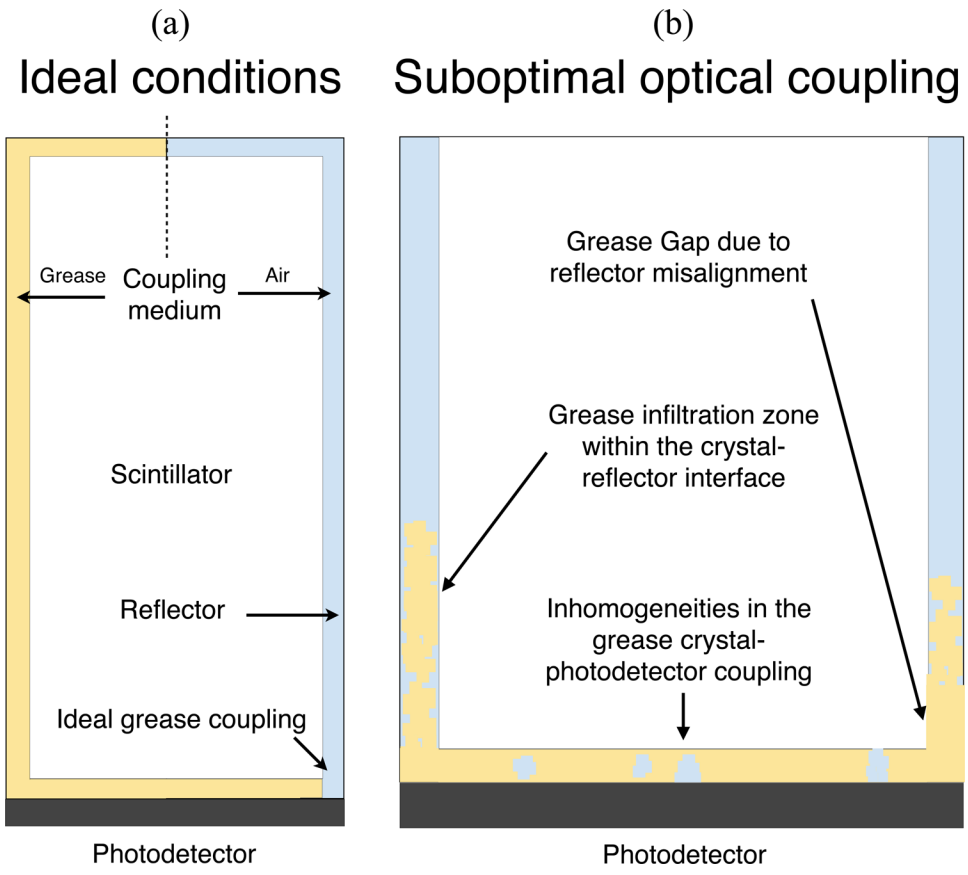

Figure 3:
Schematic view of (a) ideal crystal to photodetector and crystal to reflector couplings. (b) Several scenarios of suboptimal optical couplings. Images are not to scale.

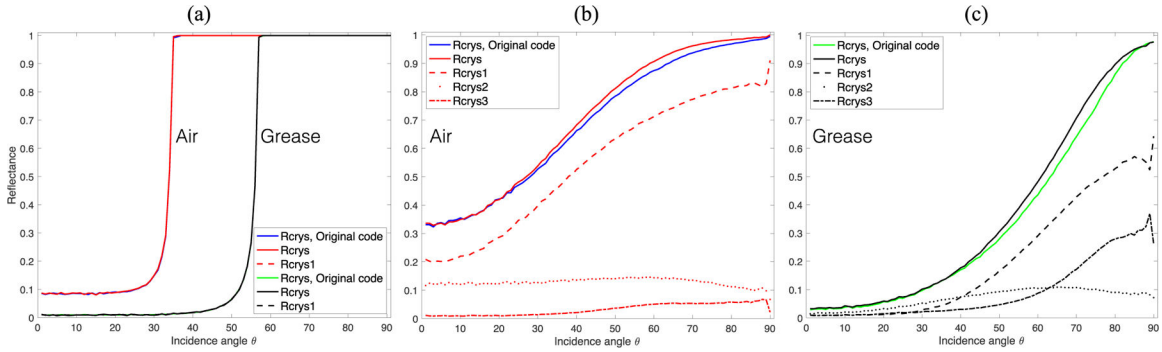

Figure 4.

(a) Reflectance of the polished surface in contact with air and grease. The reflectance obtained with the original code (solid blue and green lines, for air and grease, respectively) is superimposed to the ones obtained with the optimized code when considering all the reflected photons Rcrys (solid red and black lines, for air and grease, respectively) or only the directly reflected ones Rcrys1 (dotted red and black lines, for air and grease respectively). (b) Reflectance of the rough surface in contact with air. In blue and red, the reflectance obtained with the original and the optimized code, respectively. (c) Reflectance of the rough surface in contact with grease. In green and black, the reflectance obtained with the original and the optimized code, respectively. In the last two figures, the reflectance is computed for all the reflected photons (Rcrys), for the directly reflected (Rcrys1), reflected after one or multiple reflections (Rcrys2), or after one or multiple refractions (Rcrys3), as summarized in Figure 2.

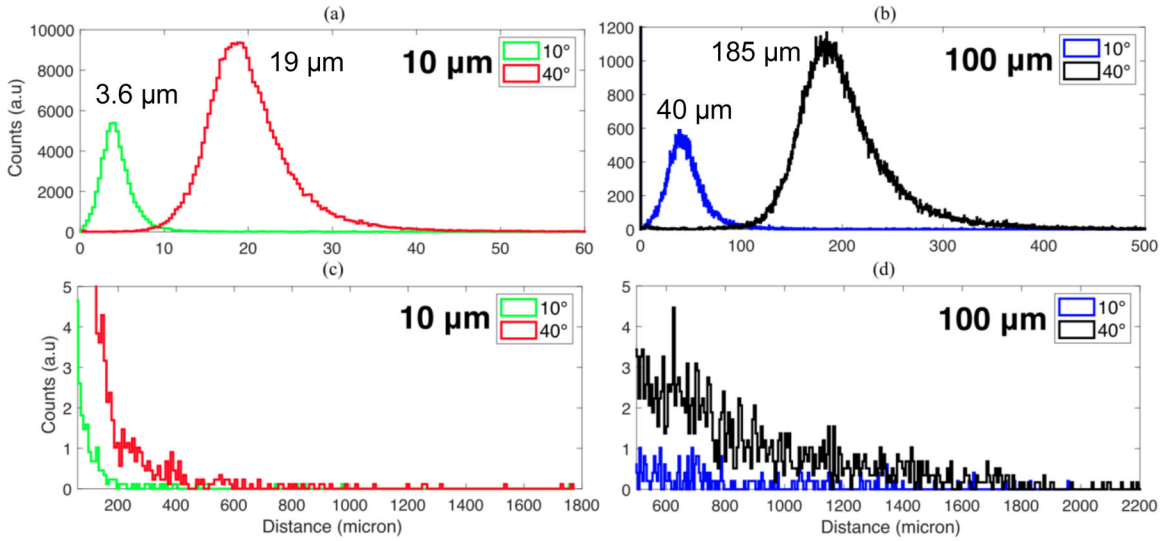

Figure 5.

Distance traveled by the photons inside the coupling, for a coupling thickness of (a-c) 10 µm and (b-d) 100 µm, for two incident angles (θ = 10° and θ = 40°). (c) and (d) zoom on the tails of the distributions (a) and (c), respectively. Note the different y-axis scales, much smaller in (c) and (d).

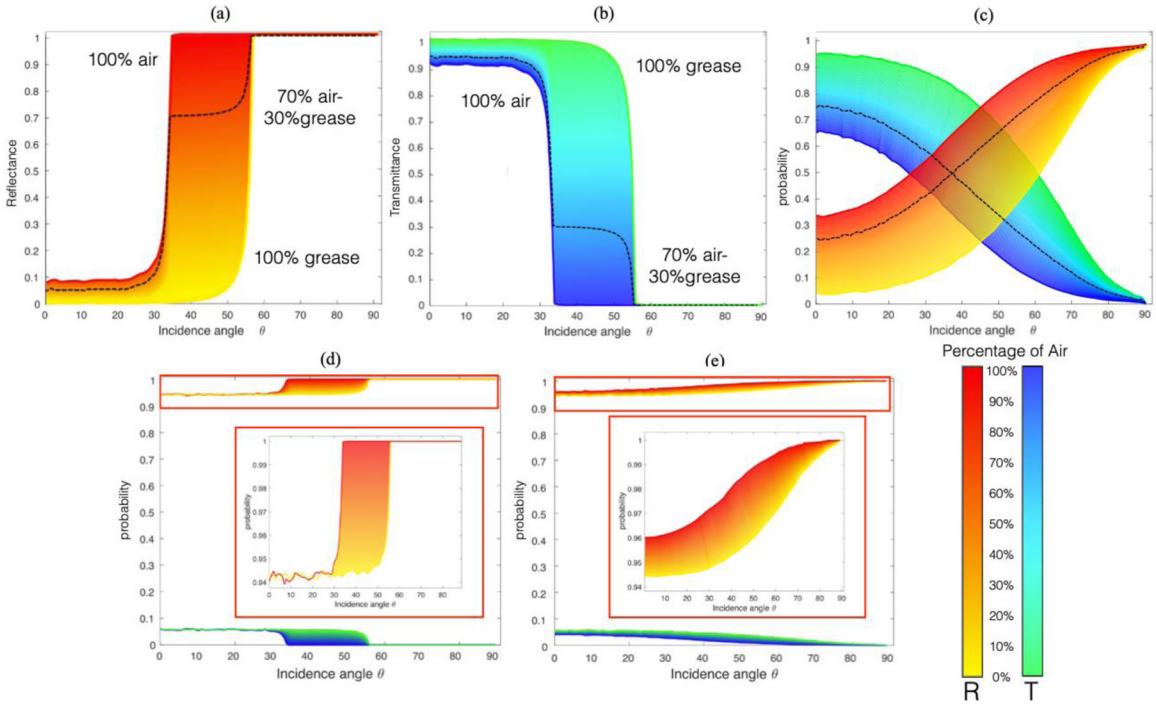

Figure 6.

(a) Polished reflectance R of the mixed LUT for air/grease ratios from 0% to 100% (red: 100% of air; yellow:100% of grease) without reflector. In black, reflectance of the mixed LUT with 70% of air and 30% of grease. (b) Corresponding polished Transmittance T (blue: 100% air; green: 100% grease; black: 70% of air) without reflector. (c) Rough reflectance and transmittance without reflector. (d) Polished surface and (e) rough surface reflectance with a mixture of air and grease in the coupling interface between the scintillator and an ESR reflector.

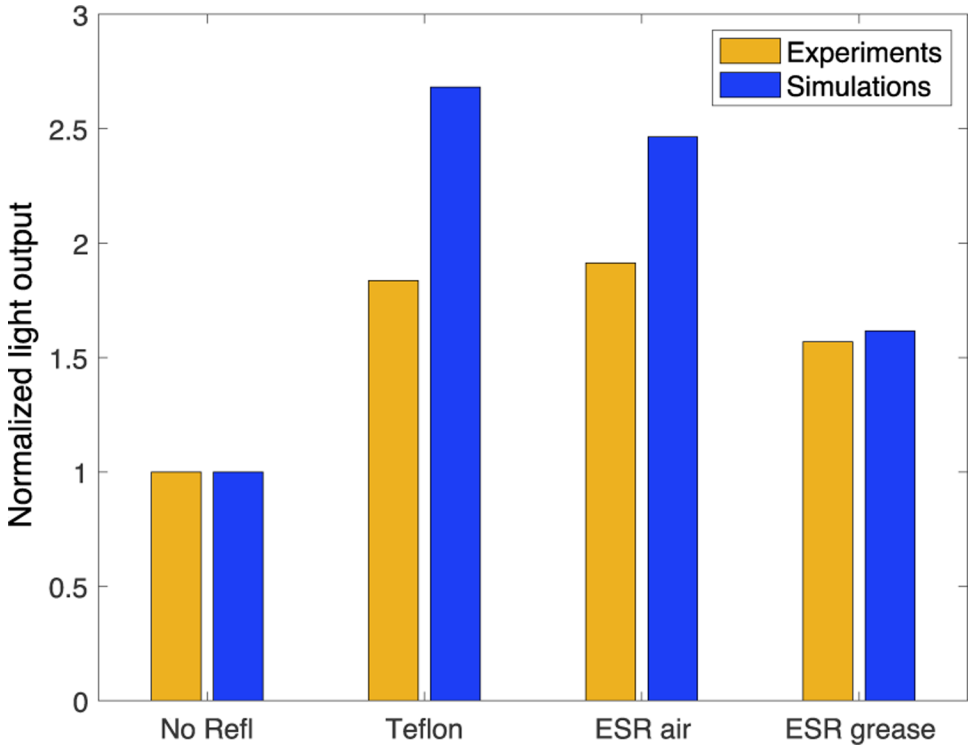

Figure 7.

Normalized light output (taken at 2 mm from the photodetector face) for rough crystals with no reflector, Teflon or ESR air-coupled or ESR grease-coupled. The simulations show an overestimation of the light output compared to the experimental results.

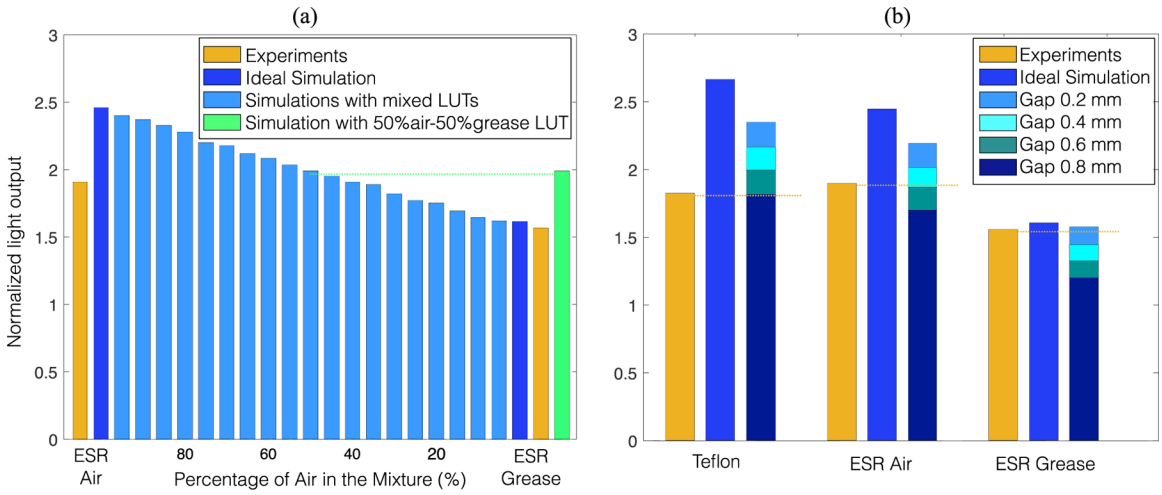

Figure 8.

(a) Normalized light output when progressively changing the relative amount of grease and air in the crystal-reflector (ESR) coupling of a rough surface along the five crystal sides (light blue). The experimental results (yellow) and the ideal simulation (blue), already shown in Figure 7, are used here for better visual comparison. (b) Normalized light output results obtained by adding small grease gaps of 0.2–0.8 mm close to the photodetector face (shades of light blue), for rough crystal coupled with Teflon, ESR-air and ESR-grease. The light output decreases by 12% and 32% in the case of Teflon, 10% and 32% with ESR-air and 2% and 25% with ESR-grease, for a 0.2 and a 0.8 mm gap, respectively.

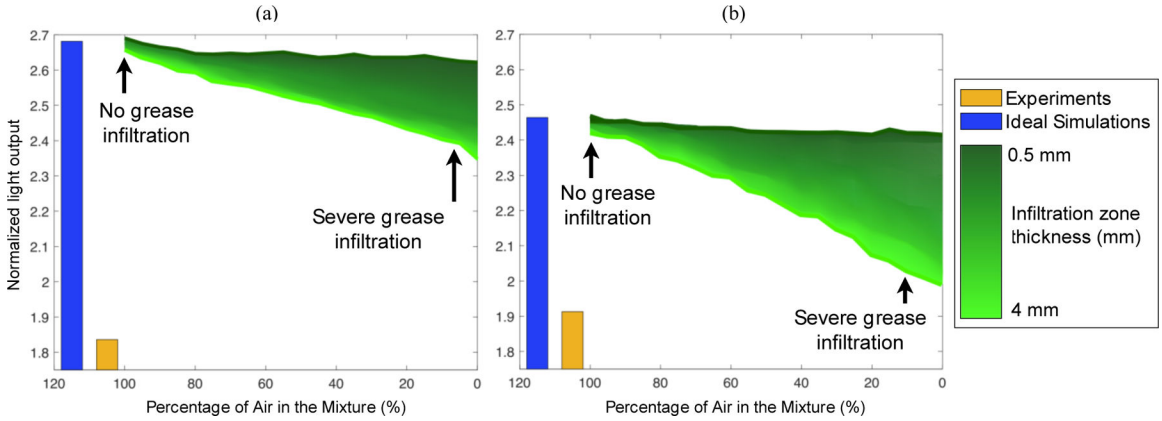

Figure 9.

Normalized light output obtained with (a) Teflon-air and (b) ESR-air when testing several infiltration zones on the sides of the crystal (from 0.5 mm to 4 mm) filled with a mixture of air and grease (from 100% to 0% of air in the air-grease mixture). The results are compared to the ideal simulation and the experiments. A mixture with 0% of air represents a complete grease infiltration within the infiltration zone. Note the limited scale on the y axis.

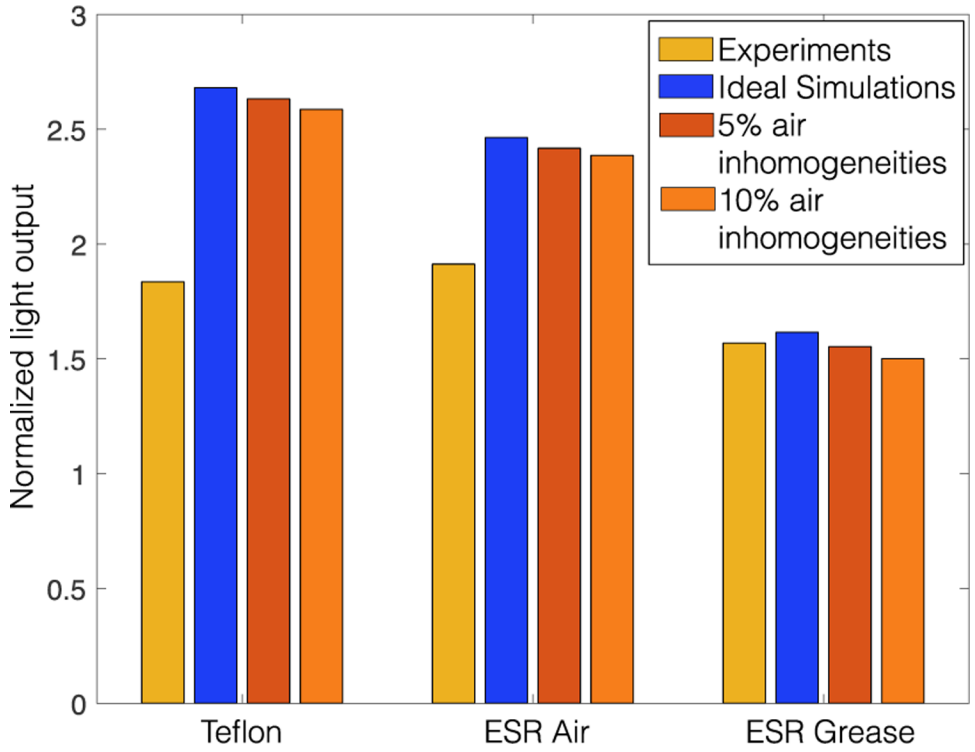

Figure 10.
Normalized light output when adding air impurities in the crystal-photodetector grease coupling (5% and 10%).

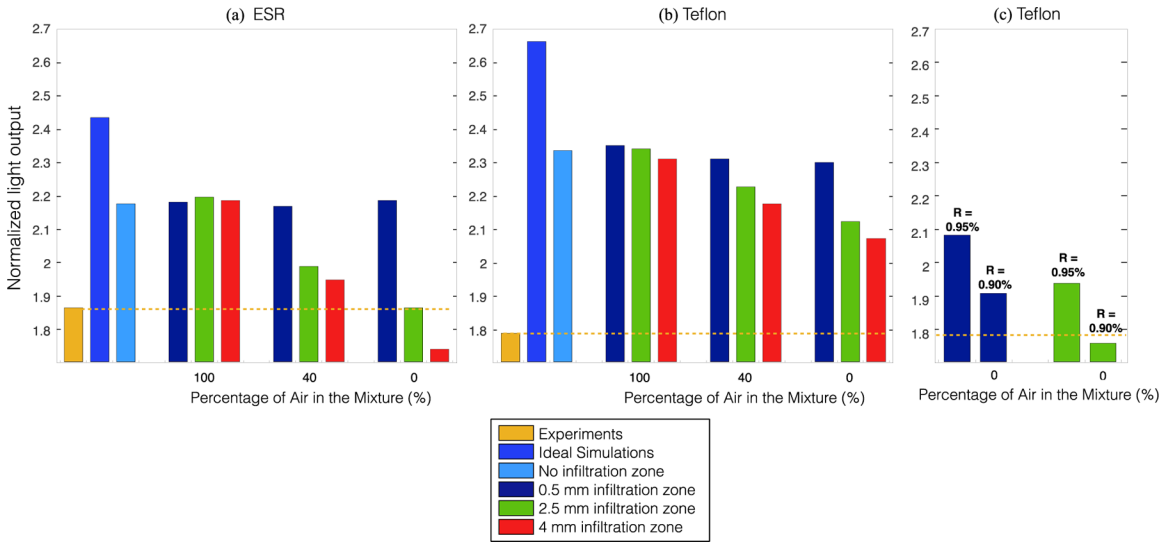

Figure 11:

Normalized light output obtained for ESR-air (a) and Teflon (b). Results obtained for three infiltration zones with different degrees of infiltration and a 0.2 mm grease gap are compared with experimental results (yellow), ideal simulation (blue), and simulation with only a 0.2 mm gap (light blue, configuration 2 Table 1). (c) Normalized light output obtained with Teflon when decreasing its reflectivity of 95% and 90%.

Table 1.

Configurations studied to investigate different suboptimal optical photodetector-crystal and reflector-crystal couplings: the presence of inhomogeneities in the crystal-photodetector coupling, the presence of a small gap in contact with grease, and infiltration of grease in the crystal-reflector coupling.

Config.	Reflector	Reflector coupling	Photodetector coupling	Gap of grease (mm)	Infiltration range
Ideal	No reflector & ESR &Teflon	Air & Grease	Grease	NO	NO
1	ESR	Mixtures of Air and Grease (from 0% to 100%)	Grease	NO	NO
2	Teflon & ESR	Air & Air/Grease	Grease	0.2, 0.4, 0.6, 0.8	NO
3	Teflon & ESR	Air	Grease	NO	Several mm and Mixtures tested.
4	Teflon & ESR	Air & Air/Grease	Mixtures of Air and Grease (5%, 10%)	NO	NO
5	Teflon & ESR	Air	Grease	0.2	Several mm and Mixtures tested.
6	Teflon & ESR	Air	Mixtures of Air and Grease (5%)	0.2	Several mm and Mixtures tested.